J. Membrane Biol. 92, 227–236 (1986)

The Journal of
Membrane Biology
© Springer-Verlag New York Inc. 1986

Calcium-Dependent Sodium Currents in *Paramecium*: Mutational Manipulations and Effects of Hyper- and Depolarization

Yoshiro Saimi
Laboratory of Molecular Biology, University of Wisconsin-Madison, Madison, Wisconsin 53706

Summary. The membrane of *Paramecium* generates a Ca-dependent Na current upon depolarization. There is, however, also a Na current upon hyperpolarization in this membrane. The second Na current was analyzed under voltage clamp and found to have properties identical to those of the first. Both currents could be carried by Na and Li ions and not by K, Cs or choline ion. They were eliminated by either EGTA injection into the cell or Ca removal from the bath. Both currents were eliminated by a single-gene mutation, *fast-2*, that had no effect on Ca currents. These findings strongly suggest that these two currents are through the same Ca-dependent Na conductance. A hyperpolarization-induced Ca current was also identified, which served to activate the second Na current. These observations support a model that the *Paramecium* membrane has two Ca channels with different voltage dependencies and only one Na channel, which is elicited by a rise of the internal free Ca^{2+} concentration. The function of the Ca-dependent Na conductance is discussed.

Key Words *Paramecium* · mutants · Ca-dependent current · Na current

Introduction

As in neurons, electrogenesis in *Paramecium* is the result of complex interactions of membrane currents. Whereas a current elicited by depolarization may participate in membrane excitation, functions of hyperpolarization-induced currents are less obvious. They may serve to regulate the resting membrane potential upon encountering different external ionic environments or be involved in the control of firing rate of action potentials as in the bursting neurons (Conner & Stevens, 1971).

Upon depolarization of the *Paramecium* membrane under voltage clamp, voltage-activated Ca and K currents and a Ca-activated K current have been recorded (*see* for review Kung & Saimi, 1982). In the presence of external Na^+, a Na current ($I_{Na,d}$) has been observed with depolarizing voltage steps (Saimi & Kung, 1980). A ^{22}Na influx has also been shown to be related with depolarization (Hansma, 1979). Like the Ca-activated K current, $I_{Na,d}$ is triggered by internal Ca^{2+} entering the cytoplasm through the Ca channel. In the presence of external Na^+ a hyperpolarization also induces an additional current noted in the previous work (Saimi & Kung, 1980).

Further study of these Na currents was hindered in the past by the presence of the K currents. $I_{Na,d}$ was first revealed with a mutant, whose Na current is enhanced (Saimi & Kung, 1980) but can only be examined at low levels of depolarization where the K-current activation is negligible. Recent success in suppressing the K currents using internally applied Cs^+ and external TEA^+ (Hinrichsen & Saimi, 1984) now allows a detailed analysis of these Na currents.

This report describes the current upon hyperpolarization in the presence of Na^+. This current has many similarities to the Ca-dependent Na current upon depolarization ($I_{Na,d}$). A Ca current upon hyperpolarization that is responsible for the activation of this Na current is discovered. This report also characterizes *fast-2* mutation as a null mutation of the Ca-dependent Na currents.

Materials and Methods

Stocks and Culture

Genetically homozygous stocks of *P. tetraurelia, Dancer* (d4-623; Hinrichsen, Saimi & Kung, 1984) and *fast-2* (d4-91; Kung, Chang, Satow, Van Houten & Hansma, 1975), were derived from the wild type (51s). A trichocyst-nondischarge mutant, *nd-6* (a gift of K. Aufderheide, *see* Sonneborn, 1975), was used together with the above mutants in order to avoid trichocyst discharge due to irritation, which makes penetration with electrodes more difficult and weakens the cell. *nd-6* has no detectable behavioral or electrophysiological abnormality. Thus, double mutants, (*Dancer*)-(*nd*-6), (*fast*-2)-(*nd*-6), and a triple mutant, (*Dancer*)-(*fast*-2)-(*nd*-6), were genetically constructed and veri-

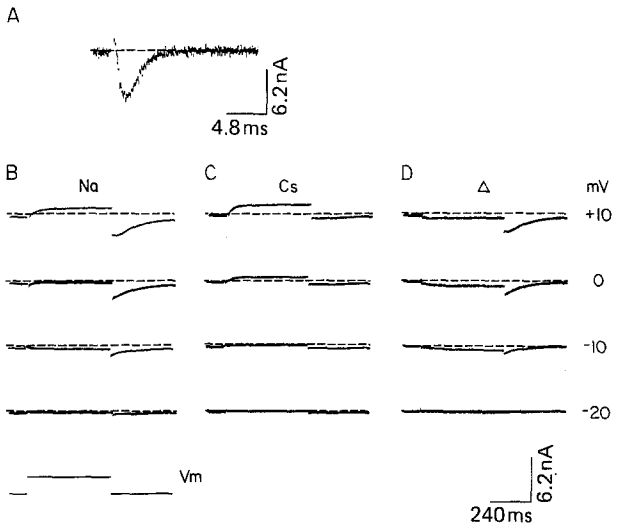

Fig. 1. The depolarization-activated Ca current and Ca-dependent Na current in wild-type *Paramecium tetraurelia* under voltage clamp. (*A*) Ca current activated by depolarization to −5 mV from the holding level of −40 mV in the Cs solution. K currents were suppressed with internal Cs^+ and external TEA^+. (*B-D*) Families of membrane currents upon 500-msec depolarization (step voltages from −40 mV indicated on the right) in the presence of 8 mM Na^+ in the bath (*B*) and those in the presence of Cs^+ (*C*) from the same cell. Comparisons would be made between the membrane currents in the presence of Na^+ and Cs^+. (*D*) Electronic subtractions of *C* from *B* to show the inward currents during the depolarization and the tails upon repolarization due to the presence of Na^+. All traces in this and following figures are presented without leakage correction. Dashed lines indicate zero current levels

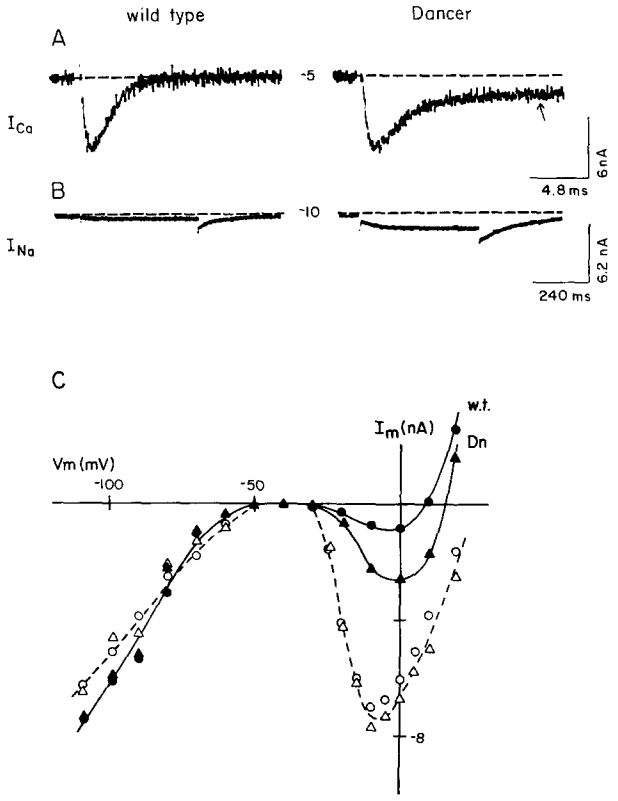

Fig. 2. The Ca and Na currents in wild type and *Dancer*. (*A*) Ca currents from the wild type (left) and *Dancer* mutant (right) activated by depolarization steps to −5 mV in the choline solution. The Ca current in the wild type inactivated very rapidly whereas that in the *Dancer* mutant showed less complete inactivation (arrow), leaving a greater residual Ca^{2+} current. (*B*) Membrane currents from the wild type (left) and the *Dancer* mutant (right) by depolarization steps to −10 mV in the Na solution. (*C*) *I-V* plots showing the peak Ca currents from the wild type (open circles) and the *Dancer* mutant (open triangles) induced by depolarizations from −40 mV. The currents at 500 msec during depolarization steps in the presence of Na^+ are plotted for the wild type (filled circles) and the *Dancer* mutant (filled triangles). In the hyperpolarization region (left of −40 mV), peak currents (open symbols) and late currents at 500 msec (filled symbols) during voltage steps in the presence of Na^+ are also shown for the wild type (circles) and the *Dancer* mutant (triangles). All points of *I-V* relations in this and the following figures are plotted after leakage correction

fied by conventional methods (Sonneborn, 1975). "Wild type," "*Dancer*," "*fast-2*" and "(*Dancer*)-(*fast-2*) *double mutant*" in this paper refer to the derived stocks all having the *nd-6* background. The cells were grown and prepared as previously described (Hinrichsen & Saimi, 1984).

Electrophysiological Measurements

The procedure of current measurement under voltage clamp was that described by Hinrichsen and Saimi (1984). The electrodes were filled with 4 M CsCl, and their resistances were approximately 20 MΩ. The holding potential was −40 mV. The membrane current was filtered at 2 kHz; for the slow events it was filtered again at 1 kHz with 8-pole Bessel function. A linear leakage current was estimated with small hyperpolarization steps and subtracted before plotting *I-V* curves.

The solutions contained 1 Ca^{2+}, 10 TEA^+ (tetraethylammonium), 0.01 $EDTA^{2-}$, and 1 HEPES (in mM) at pH 7.2-7.4. Eight mM of Cs^+, Na^+, Li^+, K^+, or $choline^+$ was added to the above basic composition to form the Cs solution, Na solution, etc. In the case where there was no added monovalent cation (the monovalent-cation-free solution), 10 mM TEA^+ was omitted from the basic solution. Chloride was the counter ion in all cases, except for the OH^- used to adjust the pH. All salts were of reagent grade. The experiments were performed at room temperatures of 20–23°C.

Results

The Ca-Dependent Na Current upon Depolarization in the Wild Type and *Dancer* Mutant

A depolarization from the holding level of −40 to −5 mV elicited in the wild type an inward Ca

current which peaked within 5 msec and then inactivated rapidly to a very low level in the presence of 1 mM Ca^{2+} (Fig. 1*A*). Because of the use of Cs^+-filled electrodes and addition of external TEA^+, K currents were greatly reduced (Hinrichsen & Saimi, 1984). When the bath also contained 8 mM Na^+, a separate inward current slowly developed and sustained over the entire step depolarization of longer than 500 msec (Fig. 1*B* at −10 mV for the clearest case; Saimi & Kung, 1980). It was followed by a large tail inward current upon repolarization which approximated a single exponential with a 260-msec time constant except at the very early times. Such an inward current and its tail were not observed when 8 mM Cs^+ (Fig. 1*C*) or choline$^+$ (*not shown*) was substituted for Na^+. As confirmed below, this slowly developing inward current and its tail are the Ca-dependent Na current (Saimi & Kung, 1980). This current will be called $I_{Na,d}$ in this paper. Subtraction of the current in the Cs solution from that in the Na solution (Fig. 1*D*) shows the difference, indicating the profile of $I_{Na,d}$ activation and deactivation.

The Ca channels activated by depolarization are shut down by the rise of the internal free Ca concentration (Brehm, Eckert & Tillotson, 1980). We have reported that this inactivation is weaker in the *Dancer* mutation, resulting in a larger Ca current sustained throughout depolarization (Hinrichsen & Saimi, 1984). As $I_{Na,d}$ is dependent on internal Ca (below), $I_{Na,d}$ should be magnified in *Dancer*. Figure 2*A* shows the Ca currents in the choline solution from the wild type (left) and that from *Dancer* (right). The sustained Ca current in the *Dancer* mutant was larger (arrow) than in the wild type, although the peak Ca currents after subtraction of leak current were the same (the third column of Table 1). The maximal sustained Ca currents at the end of a 500-msec depolarization in the choline solution after leakage correction are listed in the fourth column. As will be described later, choline$^+$ or Cs^+ does not permeate the Ca-dependent Na channel (it will be called a channel in this paper though the permeation mechanism may be otherwise).

The membrane current at 500 msec in the presence of Na^+ was also larger in *Dancer* (Fig. 2*B*, right) than in the wild type (left) as was the tail current. Note that a late inward membrane current in the presence of Na^+ starts to appear very slowly after the transient surge of the Ca current, which lasts for only less than 10 msec. Filled symbols in Fig. 2*C* show the membrane currents at 500 msec plotted against the voltage steps. The late membrane current in the depolarization half (steps from −40 mV) was larger for *Dancer* (filled triangles) than for the wild type (filled circles, also *see* Table 1). Although the late membrane current certainly included at least the Ca current and $I_{Na,d}$, the prominent tail after return from depolarization voltages (<+10 mV) to the holding level of −40 mV was also larger in the *Dancer* mutant than in the wild type (Fig. 2*B*). This slow tail was strictly associated with $I_{Na,d}$ and not with the Ca current (Hinrichsen & Saimi, 1984). Through this and a previous work (Hinrichsen & Saimi, 1984), no other alterations were noticed in the *Dancer* mutant besides the depolarization-activated Ca current and its consequences such as $I_{Na,d}$. Because of the larger but otherwise apparently normal $I_{Na,d}$ in *Dancer* at the intermediate voltage range less than +10 mV, I decided to use *Dancer* mutant to characterize $I_{Na,d}$ further. Using *Dancer* mutant, a large $I_{Na,d}$ was elicited with a relatively low depolarization, which avoided an unnecessary harm to the cell.

Table 1. Membrane currents upon depolarization from three strains of *Paramecium* in different solutions

Stain	Solution	$I_{Ca,peak}$ (nA)	$I_{500msec}$ (nA)	*n*
Wild type	Cs	−7.4 ± 0.6	−0.3 ± 0.1	8
	Choline	−7.3 ± 0.6	−0.2 ± 0.1	3
	Na	−7.8 ± 0.6	−1.1 ± 0.2	4
Dancer	Monovalent cation-free	−8.8 ± 1.9	−1.6 ± 0.5	4
	Cs	−7.3 ± 1.1	−0.9 ± 0.3	9
	Choline	−9.0 ± 1.6	−1.6 ± 0.3	8
	K	−5.7 ± 1.0	−0.6 ± 0.2	3
	Li	−6.8 ± 1.2	−3.0 ± 0.8	3
	Na	−7.2 ± 0.5	−3.1 ± 0.5	9
fast-2-Dancer	Choline	−7.4 ± 1.0	−0.9 ± 0.2	9
	Na	−6.3 ± 0.7	−0.8 ± 0.2	5

Peak calcium currents and currents at 400 msec during depolarization steps from −40 to −5 mV in wild type, *Dancer* mutant and (*fast*-2)-(*Dancer*) double mutant after subtraction of linear leakage (mean ± SD: *n* = number of cells). Underlined entries indicate late currents from each strain in the Na solution to facilitate comparison.

A Current in the Presence of Na^+ upon Hyperpolarization

In the absence of external Na^+, a hyperpolarization step more negative than −60 mV elicited in *Dancer* a membrane current whose characteristics and time course were complex (Fig. 3*B*). There was an inward component in the total current upon hyperpolarization that peaked at around 50 msec. The total membrane current then usually declined slightly but gradually increased again inwardly. Since I applied internal Cs^+ and external TEA^+ and also excluded K^+ from the bath, it is unlikely that the observed inward current upon hyperpolarization was a K cur-

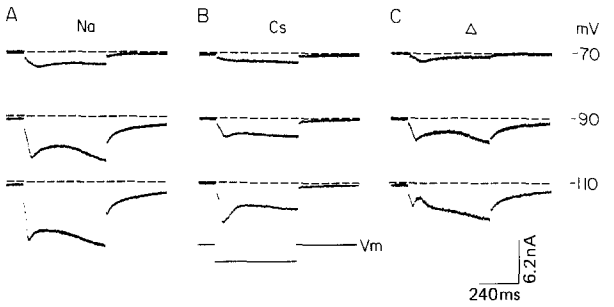

Fig. 3. Hyperpolarization-induced currents in *Dancer*. (*A*) Families of membrane currents upon 500-msec hyperpolarization (step voltages indicated on the right) in the presence of Na^+ in the bath and (*B*) those in the presence of Cs^+ from the same *Dancer* cell. (*C*) Electronic subtractions of *B* from *A* to show the differences due to the presence of Na^+

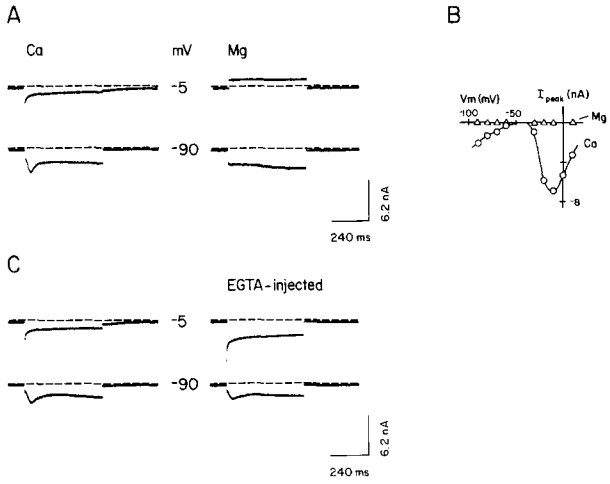

Fig. 4. Effects of Ca substitution and EGTA injection on the membrane current in the Na^+-free solution. (*A*) Effects of substitution of Mg^{2+} for Ca^{2+} on the peak currents from the *Dancer* mutant. Upper traces were induced by depolarization to −5 mV, and lower ones by hyperpolarization to −90 mV in the Na-free choline solution with Ca^{2+} (left) or Mg^{2+} (right). (*B*) The peak Ca currents upon depolarization (right to −40 mV) and the peak current upon hyperpolarization (left) in the presence of Ca^{2+} (circles) are plotted, whereas such peak currents upon both de- and hyperpolarization were not detected in the absence of Ca^{2+} (triangles). (*C*) Effects of EGTA iontophoresis (9 nA, for 1 min) into the *Dancer* mutant bathed in the choline solution. The membrane currents before (left) and after (right) the injection from the same cell are shown for depolarization (upper) and hyperpolarization steps (lower)

rent. The peak current at around 50 msec appeared to have a Ca component (*see below*).

In the presence of Na^+ in the bath, both the peak current and the later current during the step hyperpolarization (Fig. 3*A*) became larger in *Dancer*. These additional currents were therefore either due to Na^+ permeation or a stimulation of the existing currents by Na^+. The most notable change upon adding Na^+ to the bath was a large inward tail current that was seen upon return to the holding level. This tail current showed at least two exponential components, with time constants of 45 and >400 msec after a step to −90 mV. Figure 3*C* shows subtractions of the currents in Cs solution from those in the Na solution, showing the profile of the membrane current due to the presence of Na^+.

The properties of these currents from *Dancer* were identical to those from the wild type (*see* Table 2: third column for peak currents and fifth column for currents at 500 msec of voltage steps; *also see* Fig. 2*C*, left of −40 mV). This is consistent with the view that the primary defect of the *Dancer* mutation is in the depolarization-activated Ca current (Hinrichsen & Saimi, 1984) and in neither the Na channel nor the presumptive Ca current triggered by hyperpolarization (*see below*).

A Hyperpolarization-Induced Ca Current

Because the hyperpolarization-induced currents were not previously characterized in the absence of Na^+ and in the presence of the K channel blockers, it was necessary to first examine currents upon hyperpolarization without Na^+ before studying the additional currents due to Na^+. When external Ca^{2+} was replaced with Mg^{2+} in the Na^+-free solution, the peak current at approximately 50 msec upon hyperpolarization was lost (Fig. 4*A*, lower traces). The membrane currents were plotted against voltage after subtraction of a linear leakage current (Fig. 4*B*). The *I-V* relation shows the peak amplitudes for the depolarization-activated Ca current and for the hyperpolarization-induced current at around 50 msec in the presence of Ca^{2+} (circles). No such peak currents were observed in the Ca^{2+}-free Mg solution (triangles). These results indicate that the peak current upon hyperpolarization is a hitherto unknown Ca or Ca-activated conductance.

In order to test whether this peak current upon hyperpolarization was a current through a Ca channel or a current activated by internal Ca^{2+}, I injected $EGTA^{2-}$ iontophoretically into *Dancer* cells. The effect of EGTA injection on the depolarization-activated Ca current has been well established (Brehm et al., 1980). Therefore, I used this current as an indicator of the effectiveness of EGTA injection. Figure 4*C* shows current traces upon depolarization (upper) and hyperpolarization (lower). After EGTA was iontophoresed with a 9-nA current for 1 min, the sustained inward Ca current upon depolarization in the choline solution increased (upper

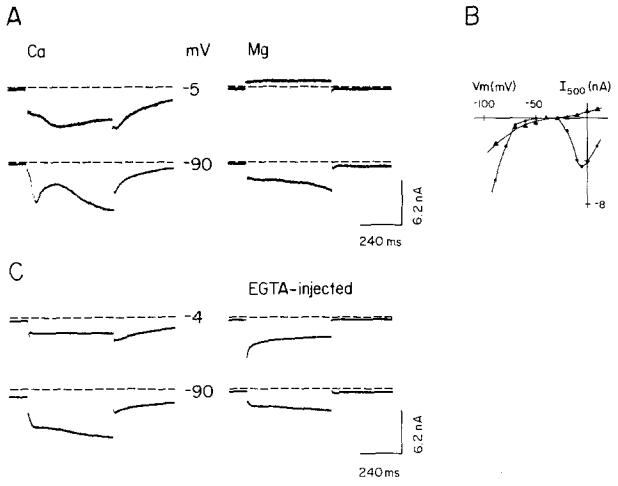

Fig. 5. Ca dependence of Na currents in *Dancer*. (*A*) Effects of substitution of Mg^{2+} for Ca^{2+} on the membrane currents from the *Dancer* mutant bathed in the solution with Na^+. (*B*) The late currents at 500 msec during voltage steps in the presence of Na^+ with Ca^{2+} (circles) or Mg^{2+} (triangles) are plotted. (*C*) Effects of EGTA injection into the *Dancer* mutant bathed in the Na solution. Except for the presence of Na^+ the procedures were similar to those for Fig. 4

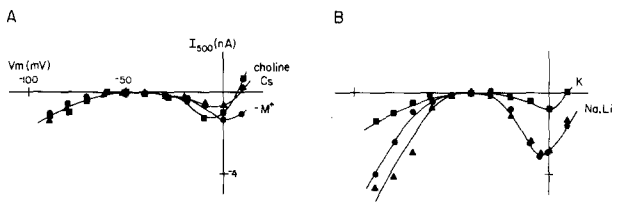

Fig. 6. *I-V* relations of membrane currents of *Dancer* cells bathed in different solutions. All solutions contained (in mM): 1 Ca^{2+}, 0.01 $EDTA^{2-}$, 1 HEPES (pH 7.2-7.4), and 10 TEA^+. TEA^+ was omitted in the monovalent-cation-free ($-M^+$) solution (*A*, circles). Eight mM of Cs^+ (*A*, triangles), $choline^+$ (squares), Na^+ (*B*: circles), Li^+ (triangles) or K^+ (squares) were added to form each of the other solutions. The late currents at 500 msec are plotted against step voltages, showing those in the Na or Li solution are larger than the rest. Choline data from one cell; Cs and $-M^+$ from the second cell; all in *B* from a third cell

right). This was due to a removal of Ca-dependent Ca-channel inactivation by effective Ca^{2+} buffering (Brehm et al., 1980). Although the peak inward current upon hyperpolarization was reduced slightly by the EGTA injection (lower right), a large portion of the peak current was not affected. This maintenance of the peak current even after EGTA injection was consistent with its being a Ca current, rather than an internal Ca^{2+}-activated current.

The Ca-substitution experiment and the EGTA-injected experiment suggest that the peak current upon hyperpolarization includes a current through a Ca conductance, which is apparently different from the depolarization-activated Ca channel in the voltage dependency.

Characterization of the Na-Induced Current upon Hyperpolarization

As shown above, the change in the membrane current by hyperpolarization upon Na^+ addition to the bath was threefold: an increase in the peak current at around 50 msec, an increase in the late current by 500 msec and the appearance of a slow inward tail current upon repolarization (Fig. 3). For the sake of clarity, the net increase due to addition of Na^+ in the total membrane current upon hyperpolarization will be collectively designated $I_{Na,h}$ hereon in this paper.

Since it has been shown that $I_{Na,d}$ upon depolarization is Ca-dependent (Saimi & Kung, 1980), I examined the Ca sensitivity of $I_{Na,h}$. Most of $I_{Na,h}$ was lost by substituting external Ca^{2+} with Mg^{2+} (Fig. 5*A*). Figure 5*B* plots the currents at 500 msec of voltage steps in the presence of Ca^{2+} (circles) and Mg^{2+} (triangles), showing that the large inward currents both upon depolarization and upon hyperpolarization were lost by substituting Ca^{2+} with Mg^{2+}. $I_{Na,h}$ was also diminished after EGTA iontophoresis with a 9-nA current for 1 min (Fig. 5*C*). Under either of these conditions, $I_{Na,d}$ was also lost. Note that the increased sustained inward current during a depolarization after EGTA injection (Fig. 5*C* upper right) was due to the sustained Ca current prevented from Ca-dependent inactivation as in Fig. 4*C*. The results indicate that $I_{Na,h}$ is activated by internal Ca^{2+} as in the case for $I_{Na,d}$.

I examined the ion selectivity of the channel responsible for $I_{Na,h}$ (Fig. 6*A* and *B*, left of −40 mV). In solutions containing K^+, Cs^+ or $choline^+$ the peak current (Table 2: third column) and the late current were smaller than $I_{Na,h}$ (Fig. 6*A*: triangles for the Cs^+, squares for $choline^+$; 6*B*: squares for K^+; *see* also Fig. 3), nor were there any clear tail currents upon repolarization, as the one associated with $I_{Na,h}$. The possible contributions of the monovalent cations were further examined by eliminating all monovalent cations from the bath solution, leaving only Ca, Cl and buffer ions. The *I-V* relation in this solution is shown in Fig. 6*A* with circles marked as $-M^+$. Except for a small shift of the voltage sensitivity upon depolarization in the absence of monovalent ions, which was perhaps due to a junction potential difference, there was little difference in the late currents during the voltage steps among the Cs, choline, K and $-M^+$ solutions (Table 2, fifth column). The peak currents (Table 2, third column)

Table 2. Membrane currents upon hyperpolarization from three strains of *Paramecium* in different solutions

Stain	Solution	I_{peak} (nA)	*n*	$I_{500msec}$ (nA)	*n*
Wild type	Cs	−2.8 ± 0.3	6	−1.7 ± 0.3	8
	Choline	−2.1 ± 1.2	3	−1.1 ± 0.4	3
	Na	−3.2 ± 1.0	3	−4.3 ± 0.5	4
Dancer	Monovalent cation-free	−1.8 ± 0.2	4	−1.0 ± 0.2	4
	Cs	−2.2 ± 0.6	8	−1.4 ± 0.4	9
	Choline	−2.0 ± 0.6	8	−1.2 ± 0.4	8
	K	−2.4 ± 0.4	3	−1.3 ± 0.4	3
	Li	−3.5 ± 1.5	3	−4.3 ± 0.8	3
	Na	−3.9 ± 0.8	7	−4.1 ± 1.1	9
fast-2-Dancer	Choline	−0.9 ± 0.4	9	−0.3 ± 0.4	9
	Na	−0.8 ± 0.2	5	−0.5 ± 0.1	5

Peak currents and currents at 500 msec during hyperpolarization steps from −40 to −90 mV in wild type, *Dancer* mutant and (*fast-2*)-(*Dancer*) double mutant after subtraction of linear leakage (mean ± SD: *n* = number of cells). Underlined entries indicate late currents from each strain in the Na solution to facilitate comparison to other entries.

as well as the tail currents (*not shown*) also showed little difference in these solutions.

When the bath had Li^+ (Fig. 6*B*, triangles) instead of Na^+ (circles), the peak current at approximately 50 msec, the late current during voltage steps, and the tail current all became as large as those of $I_{Na,h}$. The time course of the Li-induced current was very similar to that of $I_{Na,h}$.

The selectivity of the channel for $I_{Na,d}$ upon depolarization (Fig. 6*A,B* right of −40 mV) was reexamined and compared with that for $I_{Na,h}$. None of K, Cs and choline ions gave rise to an increased current amplitude during depolarization steps as large as the Na or Li current. There was no large tail current after depolarization when Cs, choline or no monovalent cation (labeled as $-M^+$) was present. However, a tail current in the K solution was observed but was less than −1.3 nA and decayed with a time constant of about 190 msec, which was faster than that of $I_{Na,d}$. Since the time course of the K tail was much different from those of Li and Na tails, it is not likely that the K tail current was going through the Na channel. Unlike molluscan Ca-activated K channels (Hermann & Gorman, 1981), the Ca-activated K channel in *Paramecium* is not effectively inhibited by external TEA^+ (Y. Saimi, *unpublished*).

The above experiments therefore showed that $I_{Na,d}$ and $I_{Na,h}$ are identical in their dependence on internal Ca^{2+} and ion selectivity. They also suggest that both currents are through the same Na channel.

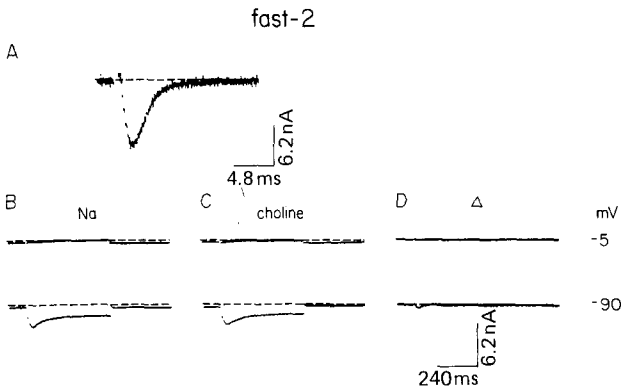

Fig. 7. Membrane currents from the *fast-2* mutant. (*A*) The Ca current by depolarization to −5mV in the choline solution. (*B*) Membrane currents upon 500-msec step de- or hyperpolarization (voltage indicated on the right) in the Na solution and (*C*) those in the choline solution. (*D*) Subtractions of the currents in the choline solution from those in the Na solution, showing little difference between them. *Compare* this figure with Figs. 1 and 3

This channel can be activated by internal Ca^{2+}, originating from two different sources, either a depolarization-induced Ca conductance or a hyperpolarization-induced one.

The *fast-2* Mutation Deletes both $I_{Na,d}$ and $I_{Na,h}$

If both $I_{Na,d}$ and $I_{Na,h}$ use the same ion channel, mutants may be found that would affect both currents at once. Null mutations are particularly useful in that they completely remove specific conductances. *Fast-2*, a single-gene mutant of *P. tetraurelia*, has been reported as behaviorally insensitive to Na^+ (Kung et al., 1975). It has also been reported not to show spontaneous action potentials in the presence of Na^+ (Satow & Kung, 1976). I therefore examined $I_{Na,d}$ and $I_{Na,h}$ of *fast-2* under voltage clamp. In the presence of Na^+ *fast-2* mutant did not have an $I_{Na,d}$ by depolarization voltage steps up to +50 mV (Fig. 7*B*, upper trace). Neither the sustained Na inward current during the depolarization step nor its tail upon return to the holding level was detected. Similarly, $I_{Na,h}$ upon hyperpolarization and its tail were also missing in *fast-2* (Fig. 7*B*, lower trace). The total membrane currents upon both de- and hyperpolarization in the presence of Na were very similar to those in Cs or choline solution (Fig. 7*C*). Subtractions of currents in the choline solution from those in the Na solution yielded almost no current that could be attributed to the presence of Na^+ (Fig. 6*D*).

Since $I_{Na,d}$ and $I_{Na,h}$ are activated by internal Ca^{2+}, it is necessary to determine whether the *fast-2* mutation also effect the Ca current upon depolariza-

tion and that upon hyperpolarization (*see* above). The depolarization-activated Ca current (Fig. 7*A*; *compare* to Fig. 1*A*) in *fast-2* mutant had a normal peak amplitude (-7.3 ± 2.4 nA: $n = 3$) and time course. That *fast-2* mutation deletes $I_{Na,d}$ and $I_{Na,h}$ almost completely and has no effect on the Ca currents was further demonstrated by examining the currents in the (*Dancer*)-(*fast-2*) double mutant. This double mutant had a larger sustained depolarization-activated Ca current exactly as the *Dancer* single mutant (Fig. 8*A* right; Hinrichsen & Saimi, 1984), but did not have significant amount of Na current upon depolarization (Fig. 8*A*, left; *B*, *I-V* relation) despite the large Ca current sustained throughout the step depolarization due to the *Dancer* defect.

The hyperpolarization-induced peak current at around 50 msec that included the hyperpolarization-induced Ca current (*see above*) in the choline or Cs solution was slightly smaller in (*Dancer*)-(*fast-2*) mutant than in the *Dancer* mutant (Fig. 8*A*, lower traces; Table 2, third column). Although this peak current became larger in *fast-2* upon a deeper hyperpolarization, no substantial $I_{Na,h}$ in *fast-2* was detected as judged by lack of tail current. The complex nature of the hyperpolarization-induced peak current at around 50 msec is discussed below.

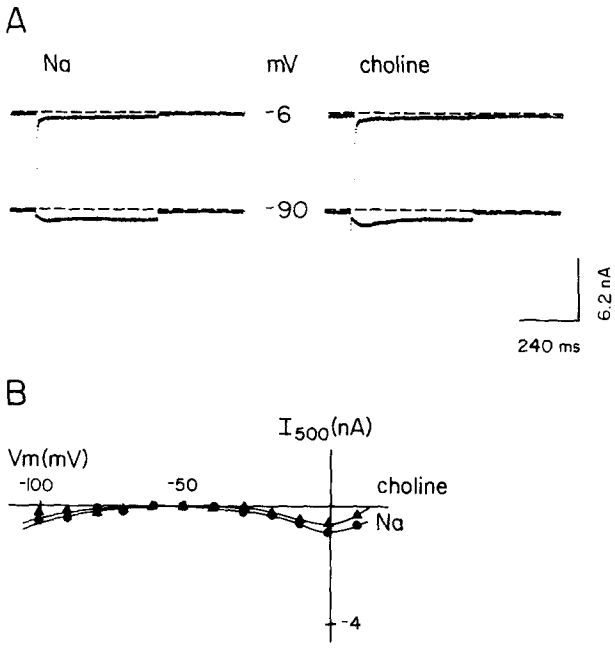

Fig. 8. Absence of the Na current in the (*fast-2*)-(*Dancer*) double mutant. (*A*) Membrane currents upon de- (upper) or hyperpolarization (lower) in the Na solution (left) and in the choline solution (right), showing little activation of the Na currents in the double mutant. (*B*) The late membrane currents at 500 msec during voltage steps in the Na solution (circles) and choline solution (triangles) are plotted against voltages. *Compare* this figure with Fig. 2*C*

Discussion

The Identity of the Na Conductances upon De- and Hyperpolarization

Three membrane currents associated with hyperpolarizations are increased by an addition of Na^+ to the bath: the large peak current at around 50 msec, the later current by 500 msec, and the slow tail current (Fig. 3). These three membrane currents are always associated. They appear when the bath has Na^+ or Li^+ (Fig. 6) and disappear when external Ca^{2+} is taken out from the bath or $EGTA^{2-}$ is injected into the cell (Fig. 5). *Fast-2* mutation removes these three currents (Figs. 7 and 8). These three currents thus appear to be of the same conductance and are collectively called $I_{Na,h}$ here.

This study shows that $I_{Na,h}$ upon hyperpolarization and the Ca-dependent Na current upon depolarization ($I_{Na,d}$), which has already been characterized (Saimi & Kung, 1980), have many common properties. (1) Both $I_{Na,d}$ and $I_{Na,h}$ conductances are permeable to Na^+ or Li^+. (2) Their activation is dependent on internal Ca^{2+}. (3) A single mutation, *fast-2*, eliminated almost all of these two currents. Therefore, these two conductances are most likely the reflection of the same molecular entity, the Ca-dependent Na channel (it will be called a channel through its actual molecular mechanism may differ). The differences in the amplitude and kinetics between the two Na currents are probably a manifestation of differences in Ca^{2+} influx or removal upon de- and hyperpolarization. Whether the Na channel has voltage dependence as in the case of the Ca-activated K channels (Moczydlowski & Latorre, 1983) has yet to be examined.

The Na channels are located on the somatic membrane because at least a fraction of them survive deciliation (Kung & Saimi, 1982). As deciliation also removes the depolarization-activated Ca current (Machemer & Ogura, 1979), whether the Na channels are also on the ciliary membrane is not known.

The Nature of the Ca-Dependent Na Conductance

A precise calculation of the Na conductance through the measurement of the reversal potential is prevented at high voltages by the activation of ion currents not fully suppressed by the K current blockers used in this study (*see*, for example, Fig. 5*B*: triangles in the depolarization half). The rever-

sal potential in 8 mM Na solution appears to be much higher than +10 mV (e.g. Fig. 1*D*). A direct comparison of the current amplitudes and tails after the voltage steps shows that Na^+ and Li^+ can pass through the Na channel well (Fig. 6). Cs, K and choline ions, on the other hand, permeate poorly. The ion selectivity of the Ca-dependent Na channel in *Paramecium* appears to be different from that of the Ca-activated, nonselective cation channels which pass Na^+ and K^+ almost equally (Colquhoun, Neher, Reuter & Stevens, 1981; Yellen, 1982; Maruyama & Petersen, 1982).

There is a very small inward tail (<0.5 nA) after both de- and hyperpolarization even in the absence of Na^+ (Fig. 4*A*). It decays with a similar time course to that of the Ca-dependent Na current and is sensitive to EGTA injection (Fig. 4*C*). As Ca^{2+} is known to pass the voltage-activated Na channel (Baker, Hodgkin & Ridgeway, 1971; Meves & Vogel, 1973), the Ca-dependent Na channel studied here may also be permeable to Ca^{2+}. Since the Ca electromotive force is expected to be much larger than that for Na^+, the small tail indicates that the Ca permeability through the Na channel is much smaller than the Na permeability.

Whereas the Na channel in *Paramecium* is dependent on internal Ca^{2+}, it has yet to be shown whether it is directly activated by binding of Ca^{2+} as is probably the case for the Ca-activated K channel. Alternatively, it could be indirectly activated by Ca-induced metabolism, for example, change in the levels of cyclic nucleotides. Na conductances in the rod outer segment (Mathews, Torre & Lamb, 1985; Fesenko, Kolesnikov & Lyubarsky, 1985) and in the molluscan neurons (Aldenhoff, Hofmeier, Lux & Swandulla, 1983; Conner & Hockberger, 1984) are activated by cyclic nucleotides. The Na channel in the rod outer segment (Capovilla, Caretta, Cervetto & Torre, 1983; Yau & Nakatani, 1984; Hodgkin, McNaughton & Nunn, 1985) and the Na conductance in *Helix* (Swandulla & Lux, 1984), however, have rather broad ion selectivity unlike the Na channel in *Paramecium*.

Although the Ca-dependent Na current could be generated by a Na-Ca exchange mechanism (Connolly & Kerkut, 1983), it is more likely that this *Paramecium* Ca-dependent Na current is through a channel with a large Li permeability. Li^+ is usually far less efficient than Na^+ for the Na-Ca exchange mechanism.

The *fast-2* Mutation

The *fast-2* mutant clearly lacks the Ca-dependent Na current upon de- and hyperpolarization. It appears that *fast-2* mutation shuts down the Na conductance. The elimination of Na current is nearly complete since the mutant's current upon hyperpolarization in the Na solution, where the driving force for Na^+ is large, is still not different from that in the Na^+-free choline solution (Figs. 7 and 8).

The depolarization-activated Ca current (Fig. 7*A*) and K currents (*data not shown*) of *fast-2* mutant are all normal. This null mutation of the Na current is particularly useful for testing the behavioral significance of the Na current as well as for examining the remaining current in the mutant.

The Ca Source upon Hyperpolarization

The existence of the Ca-dependent Na current upon hyperpolarization raises the question regarding the source for Ca^{2+}. Although the possibility of Ca^{2+} release from the internal binding sites has not been ruled out, it appears that there is a Ca influx upon hyperpolarization. The peak current upon hyperpolarization at around 50 msec appear to contain a Ca current. This peak current is removed upon substitution of external Ca^{2+} with Mg^{2+} (Fig. 4*A*) and is largely resistant to injected $EGTA^{2-}$ (Fig. 4*C*). These observations indicate that the peak current consists of both a hyperpolarization-activated Ca current and a smaller current(s) that is activated by internal Ca^{2+}. As $I_{Na,h}$ has a peak component at around 50 msec (Fig. 3) and the Na channel may be slightly permeable to Ca^{2+} (*see* above discussion), this $EGTA^{2-}$-sensitive component may be a Ca current through the Na channel. If *fast-2* mutation only affects the Na channel, the peak current at around 50 msec upon hyperpolarization in *fast-2* mutant is expected to be small (Table 2: third column) since the $EGTA^{2-}$-sensitive component of the peak current may be a Ca current through the Ca-dependent Na channels.

Behavioral Significance of the Ca-Dependent Na Currents

It has been reported that, in external Na^+ concentrations lower than 5 mM *Paramecium* actually takes up Na^+ in concentrations higher than the external Na^+ concentration (Hansma, 1979; Connolly & Kerkut, 1983). At higher Na^+ concentrations, the calculated reversal potential becomes positive, although we do not know exactly how Na^+ is regulated in different ionic media. However, at least in such experimental conditions as the Na solutions that we routinely use (Kung et al., 1975), the Na current may act to maintain the membrane depolar-

ization after a surge of the Ca current to the peak depolarization. Since the Na current is activated by the Ca^{2+} influx and the Na inward current depolarizes the membrane, which in turn maintains a small flow of the Ca current through the uninactivated Ca channels, the Ca and Na currents complete a positive feedback loop. The *N*-shaped *I-V* curve of this Na current (Fig. 2) makes this feedback inevitable. This positive feedback is usually counteracted by slower activation of the Ca^{2+}-activated K current, the absence of which further prolongs the action potential. Therefore, these three Ca^{2+}-related currents form an action potential of an intermediate length of hundreds of milliseconds under certain ionic conditions (Saimi, Hinrichsen, Forte & Kung 1983) leading to a stronger avoiding reaction. That *fast-2* mutant fails to generate such an action potential (Satow & Kung, 1976) supports this view.

The unclamped membrane can be strongly hyperpolarized by currents such as the Ca^{2+}-activated K current. The Na^+ inward current induced by hyperpolarization of the membrane is expected to depolarize the membrane. Thus, it is possible that the membrane potential bounces back to a depolarized level from a hyperpolarization, and after the long action potential goes back to a hyperpolarized level. Such an interaction of currents would cycle many times. Membrane potential oscillations each lasting about a second have been observed in *Paramecium* bathed in a solution containing Na^+ (Satow & Kung, 1974). Whether there is a conductance of the Na channel at the "resting" potential is not clear. If the "resting" Na conductance is low, oscillation of the membrane potential could be initiated by reception of a stimulation such as mechanical and chemical ones (Kung & Saimi, 1982).

I thank Dr. C. Kung for his continuous encouragement and advice during this work, and Drs. M. Gustin and B. Martinac for their critical reading of the manuscript. This work was supported by a grant, BNS-82-16149.

References

Aldenhoff, J.B., Hofmeier, G., Lux, H.D., Swandulla, D. 1983. Stimulation of a sodium influx by cAMP in *Helix* neurons. *Brain Res.* **276:**289–296.

Baker, P.F., Hodgkin, A.L., Ridgeway, E.B. 1971. Depolarization and calcium entry in squid giant axons. *J. Physiol. (London)* **218:**709–755

Brehm, P., Eckert, R., Tillotson, D. 1980. Calcium-mediated inactivation of calcium current in *Paramecium*. *J. Physiol. (London)* **306:**193–203

Capovilla, M., Caretta, A., Cervetto, L., Torre, V. 1983. Ionoic movements through light-sensitive channels of toad rods. *J. Physiol. (London)* **343:**295–310.

Colquhoun, D., Neher, E., Reuter, H., Stevens, C.F. 1981. Inward current channels activated by intracellular Ca in cultured cardiac cells. *Nature (London)* **294:**752–754

Conner, J.A., Hockberger, P. 1984. A novel membrane sodium current induced by injection of cyclic nucleotides into gastropod neurones. *J. Physiol. (London)* **354:**139–162

Conner, J.A., Stevens, C.F. 1971. Prediction of repetitive firing behavior from voltage clamp data on an isolated neurone soma. *J. Physiol. (London)* **213:**31–53

Connolly, J.G., Kerkut, G.A. 1983. Ion regulation and membrane potential in *Tetrahymena* and *Paramecium*. *Comp. Biochem. Physiol.* **76A:**1–16

Fesenko, E.E., Kolesnikov, S., Lyubarsky, A.L. 1985. Induction by cyclic GMP of cationic conductance in plasma membrane of retinal rod outer segment. *Nature (London)* **313:**310–313

Hansma, H.G. 1979. Sodium uptake and membrane excitation in *Paramecium*. *J. Cell Biol.* **81:**374–381

Hermann, A., Gorman, A.L.F. 1981. Effects of tetraethylammonium on potassium currents in a molluscan neurone. *J. Gen. Physiol.* **78:**87–110

Hinrichsen, R.D., Saimi, Y. 1984. A mutation that alters properties of the calcium channel in *Paramecium tetraurelia*. *J. Physiol. (London)* **351:**397–410

Hinrichsen, R.D., Saimi, Y., Kung, C. 1984. Mutants with altered Ca^{2+}-channel properties in *Paramecium tetraurelia:* Isolation, characterization and genetic analysis. *Genetics* **108:**545–558

Hodgkin, A.L., McNaughton, P.A., Nunn, B.J. 1985. The ionic selectivity and calcium dependence of the light-sensitive pathway in toad rods. *J. Physiol. (London)* **358:**447–468

Kung, C. 1971. Genic mutants with altered system of excitation in *Paramecium aurelia:* I. Phenotypes of the behavioral mutants. *Zeit. verg. Physiol.* **71:**142–164

Kung, C., Chang, S.-Y., Satow, Y., Van Houten, J., Hansma, H.G. 1975. Genetic dissection of behavior in *Paramecium*. *Science* **188:**898–904

Kung, C., Saimi, Y. 1982. The physiological basis of taxes in *Paramecium*. *Annu. Rev. Physiol.* **44:**519–534

Machemer, H., Ogura, A. 1979. Ionic conductances of membranes in ciliated and deciliated *Paramecium*. *J. Physiol. (London)* **296:**49–60

Maruyama, Y., Petersen, O.H. 1982. Single-channel currents in isolated patches of plasma membrane from basal surface of pancreatic acini. *Nature (London)* **299:**159–161

Mathews, H.R., Torre, V., Lamb, T.D. 1985. Effects on the photoresponse of calcium buffers and cyclic GMP incorporated into the cytoplasm of retinal rods. *Nature (London)* **313:**582–585

Meves, H., Vogel, W. 1973. Calcium inward currents in internally perfused giant axons. *J. Physiol. (London)* **235:**225–265

Moczydlowski, E., Latorre, R. 1983. Gating kinetics of Ca^{2+}-activated K^+ channels from rat muscle incorporated into planar lipid bilayers: Evidence for two voltage-dependent Ca^{2+} binding reactions. *J. Gen. Physiol.* **83:**511–542

Saimi, Y., Hinrichsen, R.D., Forte, H., Kung, C. 1983. Mutant analysis shows that the Ca^{2+}-induced K^+ current shuts off one type of excitation in *Paramecium*. *Proc. Natl. Acad. Sci. USA* **80:**5112–5116

Saimi, Y., Kung, C. 1980. A Ca-induced Na^+ current in *Paramecium*. *J. Exp. Biol.* **88:**305–325

Satow, Y., Kung, C. 1974. Genetic discussion of active electrogenesis in *Paramecium aurelia*. *Nature (London)* **247:**69–71

Satow, Y., Kung, C. 1976. A mutant of *Paramecium* with in-

creased relative resting potassium permeability. *J. Neurobiol.* **7**:325–338

Sonneborn, T.M. 1975. *Paramecium aurelia: In:* Handbook of Genetics. Vol. II, pp. 469–594. R.C. King, editor. Plenum, New York

Swandulla, D., Lux, H.D. 1984. Changes in ionic conductances induced by cAMP in *Helix* neurons. *Brain Res.* **305**:115–122

Yau, K.-W., Nakatani, K. 1984. Cation selectivity of light-sensitive conductance in retinal rods. *Nature (London)* **309**:352–354

Yellen, G. 1982. Single Ca^{2+}-activated nonselective cation channels in neuoroblastoma. *Nature (London)* **296**:357–359

Received 30 January 1986; revised 28 April 1986